JOURNAL OF GEOPHYSICAL RESEARCH

Supporting Information for "Are seasonal deposits in spring at the Martian North Pole much shallower than previously thought?"

Haifeng Xiao[1], Yuchi Xiao[2], Shu Su[1], Frédéric Schmidt[3,4], Luisa M. Lara[5], Pedro J. Gutierrez[5]

[1]Institute of Geodesy and Geoinformation Science, Technische Universität Berlin, Berlin, Germany

[2]School of Mechanical Engineering and Electronic Information, China University of Geosciences, Wuhan, China

[3]Université Paris-Saclay, CNRS, GEOPS, Orsay, France

[4]Institut Universitaire de France (IUF), Paris, France

[5]Instituto de Astrofísica de Andalucía (IAA-CSIC), Granada, Spain

Contents of this file

Table S1: HiRISE Images Adopted, Solar and Slope Properties, and Depth Results for Ice Block 1

Image ID*	Date	Solar Longitude	Mars Year Season	Solar Condition		Slope Condition		Ice Block Height [m]	Snow Depth [m]
				elevation	azimuth	magnitude	aspect		
PSP_007710	19 Mar 2008	47.0°	MY29 sp.	23°	192.7°	4.7°	64.8°	1.19	0.12
PSP_009648	17 Aug 2008	113.9°	**MY30 su.**	28°	200.6°	13.0°	115.8°	1.31	NA
ESP_016228	12 Jan 2010	36.6°	MY30 sp.	20°	189.2°	10.0°	110.0°	0.92	0.34
ESP_016426	27 Jan 2010	43.6°	MY30 sp.	22°	196.2°	10.0°	110.0°	1.06	0.20
ESP_016439	28 Jan 2010	44.0°	MY30 sp.	22°	191.1°	13.0°	115.8°	1.08	0.18
ESP_016505	02 Feb 2010	46.3°	MY30 sp.	23°	193.4°	9.6°	94.1°	1.04	0.22
ESP_016650	13 Feb 2010	51.3°	MY30 sp.	24°	192.8°	10.0°	110.0°	1.16	0.10
ESP_016716	19 Feb 2010	53.6°	MY30 sp.	25°	195.0°	10.0°	110.0°	1.19	0.07
ESP_017863	19 May 2010	92.7°	**MY30 su.**	30°	194.8°	12.8°	103.7°	1.31	NA
ESP_018905	08 Aug 2010	130.0°	**MY30 su.**	23°	205.7°	6.8°	95.3°	1.23	NA
ESP_019222	02 Sep 2010	142.1°	**MY30 su.**	19°	221.4°	6.8°	95.3°	1.26	NA
ESP_024654†	30 Oct 2011	22.7°	MY31 sp.	14°	186.2°	12.3°	94.9°	0.85	0.34
ESP_025010	27 Nov 2011	35.4°	MY31 sp.	19°	188.4°	12.3°	94.9°	0.87	0.31
ESP_025221	13 Dec 2011	42.8°	MY31 sp.	22°	190.4°	12.8°	103.7°	0.95	0.24
ESP_025577	10 Jan 2012	55.1°	MY31 sp.	25°	191.4°	13.7	108.7	1.00	0.18
ESP_027674	21 Jun 2012	128.3°	**MY31 su.**	24°	206.4°	10.0°	110.0°	1.18	NA
ESP_033713†	05 Oct 2013	31.4°	MY32 sp.	18°	189.3°	13.4°	97.8°	0.95	0.14
ESP_033766	09 Oct 2013	33.3°	MY32 sp.	18°	196.8°	9.3°	77.5°	0.88	0.20
ESP_034043	31 Oct 2013	43.0°	MY32 sp.	22°	201.1°	13.4°	97.8°	0.85	0.24
ESP_034254	16 Nov 2013	50.3°	MY32 sp.	24°	202.8°	12.8°	103.7°	0.99	0.09
ESP_034399	27 Nov 2013	55.3°	MY32 sp.	25°	202.6°	11.3°	85.8°	1.07	0.01
ESP_036535	13 May 2014	129.9°	**MY32 su.**	24°	205.2°	11.3°	85.8°	1.08	NA
ESP_052306	23 Sep 2017	64.7°	MY34 sp.	27°	193.2°	11.3°	85.8°	1.12	0.02
ESP_053875	23 Jan 2018	119.1°	**MY34 su.**	27°	196.4°	12.3°	94.9°	1.14	NA
ESP_060126	25 May 2019	30.1°	MY35 sp.	17°	187.7°	12.2°	93.1°	0.68	0.46
ESP_069095	23 Apr 2021	35.5°	MY36 sp.	19°	198.0°	11.3°	85.8°	0.84	0.30
ESP_069834	19 Jun 2021	61.0°	MY36 sp.	26°	213.8°	11.3°	85.8°	1.04	0.10
ESP_069992	02 Jul 2021	66.4°	MY36 sp.	27°	208.1°	11.3°	85.8°	1.04	0.10

* Image ID should be suffixed with "_2650". † marks the images with a grid size of 0.50 m, while the rest of them feature a better resolution of 0.25 m. Note that the solar azimuth is with respect to the North Pole while the slope aspect is defined as the angle with respect to the map north. sp. is the abbreviation for spring and su. for summer. Summer images used to derive the reference heights are marked in bold.

Table S2: HiRISE Images Adopted, Solar and Slope Properties, and Depth Results for Ice Block 2

Image ID*	Date	Solar Longitude	Mars Year Season	Solar Condition		Slope Condition		Ice Block Height [m]	Snow Depth [m]
				elevation	azimuth	magnitude	aspect		
PSP_007710	19 Mar 2008	47.0°	MY29 sp.	23°	192.7°	1.0°	295.9°	1.16	0.23
PSP_007763	23 Mar 2008	48.9.0°	MY29 sp.	23°	192.7°	2.1°	330.4°	1.26	0.12
PSP_009648	17 Aug 2008	113.9°	**MY29 su.**	28°	200.6°	3.0°	346.9°	1.40	NA
PSP_010097	21 Sep 2008	130.3°	**MY29 su.**	23°	218.6°	2.9°	324.7°	1.36	NA
ESP_016228	12 Jan 2010	36.6°	MY30 sp.	20°	189.2°	2.1°	330.4°	1.04	0.28
ESP_016426	27 Jan 2010	43.6°	MY30 sp.	22°	196.2°	3.0°	346.9°	1.09	0.23
ESP_016439	28 Jan 2010	44.0°	MY30 sp.	22°	191.1°	1.0°	295.9°	1.12	0.19
ESP_016505	02 Feb 2010	46.3°	MY30 sp.	23°	193.4°	3.0°	346.9°	1.14	0.17
ESP_016650	13 Feb 2010	51.3°	MY30 sp.	24°	192.8°	3.0°	346.9°	1.19	0.12
ESP_016716	19 Feb 2010	53.6°	MY30 sp.	25°	195.0°	3.0°	346.9°	1.17	0.14
ESP_017217	30 Mar 2010	70.7°	MY30 sp.	28°	195.0°	3.0°	346.9°	1.19	0.12
ESP_017863	19 May 2010	92.7°	**MY30 su.**	30°	194.8°	2.6°	296.3°	1.37	NA
ESP_018905	08 Aug 2010	130.0°	**MY30 su.**	23°	205.7°	3.4°	347.6°	1.26	NA
ESP_019222	02 Sep 2010	142.1°	**MY30 su.**	19°	221.4°	3.4°	347.6°	1.32	NA
ESP_024654†	30 Oct 2011	22.7°	MY31 sp.	14°	186.2°	2.1°	330.4°	0.76	0.56
ESP_025010	27 Nov 2011	35.4°	MY31 sp.	19°	188.4°	3.0°	346.9°	1.02	0.30
ESP_025221	13 Dec 2011	42.8°	MY31 sp.	22°	190.4°	2.1°	330.4°	1.15	0.17
ESP_025577	10 Jan 2012	55.1°	MY31 sp.	25°	191.4°	2.9°	324.7°	1.27	0.05
ESP_027674	21 Jun 2012	128.3°	**MY31 su.**	24°	206.4°	3.0°	346.9°	1.32	NA
ESP_033476†	17 Sep 2013	22.9°	MY32 sp.	14°	197.3°	3.0°	346.9°	0.91	0.41
ESP_033713†	05 Oct 2013	31.4°	MY32 sp.	18°	189.3°	3.0°	346.9°	1.02	0.30
ESP_033766	09 Oct 2013	33.3°	MY32 sp.	18°	196.8°	2.1°	330.4°	1.03	0.29
ESP_034043	31 Oct 2013	43.0°	MY32 sp.	22°	201.1°	2.1°	330.4°	1.01	0.31

Image ID*	Date	Solar Longitude	Mars Year Season	Solar Condition		Slope Condition		Ice Block Height [m]	Snow Depth [m]
				elevation	azimuth	magnitude	aspect		
ESP_034610	14 Dec 2013	62.5°	MY32 sp.	27°	205.0°	2.6°	296.3°	1.13	0.19
ESP_053730	12 Jan 2018	113.9°	**MY34 su.**	28°	197.4°	2.1°	330.4°	1.36	NA
ESP_069095	23 Apr 2021	35.5°	MY34 sp.	19°	198.0°	3.0°	346.9°	0.89	0.47
ESP_069649	5 Jun 2021	54.7°	MY34 sp.	25°	202.0°	2.1°	330.4°	1.19	0.17

* Image ID should be suffixed with "_2650". † marks the images with a grid size of 0.50 m, while the rest of them feature a better resolution of 0.25 m. Note that the solar azimuth is with respect to the North Pole while the slope aspect is defined as the angle with respect to the map north. sp. is the abbreviation for spring and su. for summer. Summer images used to derive the reference heights are marked in bold.

Table S3: HiRISE Images Adopted, Solar and Slope Properties, and Depth Results for Ice Block 3

Image ID*	Date	Solar Longitude	Mars Year Season	Solar Condition		Slope Condition		Ice Block Height [m]	Snow Depth [m]
				elevation	azimuth	magnitude	aspect		
PSP_007710	19 Mar 2008	47.0°	MY29 sp.	23°	192.7°	4.7°	55.2°	1.58	0.22
PSP_007763	23 Mar 2008	48.9.0°	MY29 sp.	23°	192.7°	4.7°	55.2°	1.59	0.20
PSP_009648	17 Aug 2008	113.9°	**MY29 su.**	28°	200.6°	5.9°	52.9°	1.85	NA
PSP_010097	21 Sep 2008	130.3°	**MY29 su.**	23°	218.6°	4.7°	55.2°	1.75	NA
ESP_016228	12 Jan 2010	36.6°	MY30 sp.	20°	189.2°	5.9°	52.9°	1.44	0.34
ESP_016426	27 Jan 2010	43.6°	MY30 sp.	22°	196.2°	5.9°	52.9°	1.50	0.29
ESP_016439	28 Jan 2010	44.0°	MY30 sp.	22°	191.1°	5.9°	52.9°	1.47	0.31
ESP_016505	02 Feb 2010	46.3°	MY30 sp.	23°	193.4°	5.9°	52.9°	1.53	0.25
ESP_016650	13 Feb 2010	51.3°	MY30 sp.	24°	192.8°	5.9°	52.9°	1.52	0.26
ESP_016716	19 Feb 2010	53.6°	MY30 sp.	25°	195.0°	5.9°	52.9°	1.55	0.23
ESP_017217	30 Mar 2010	70.7°	MY30 sp.	28°	195.0°	4.7°	55.2°	1.59	0.19
ESP_017863	19 May 2010	92.7°	**MY30 su.**	30°	194.8°	4.7°	55.2°	1.90	NA
ESP_018905	08 Aug 2010	130.0°	**MY30 su.**	23°	205.7°	5.9°	52.9°	1.75	NA
ESP_019222	02 Sep 2010	142.1°	**MY30 su.**	19°	221.4°	5.9°	52.9°	1.70	NA
ESP_024654†	30 Oct 2011	22.7°	MY31 sp.	14°	186.2°	7.5°	53.0°	1.28	0.45
ESP_024865	16 Nov 2011	30.3°	MY31 sp.	17°	188.6°	5.9°	52.9°	1.31	0.42

Image ID*	Date	Solar Longitude	Mars Year Season	Solar Condition		Slope Condition		Ice Block Height [m]	Snow Depth [m]
				elevation	azimuth	magnitude	aspect		
ESP_025010	27 Nov 2011	35.4°	MY31 sp.	19°	188.4°	5.9°	52.9°	1.42	0.30
ESP_025221	13 Dec 2011	42.8°	MY31 sp.	22°	190.4°	6.4°	45.0°	1.50	0.22
ESP_025577	10 Jan 2012	55.1°	MY31 sp.	25°	191.4°	5.9°	52.9°	1.57	0.21
ESP_027674	21 Jun 2012	128.3°	**MY31 su.**	24°	206.4°	5.6°	54.5°	1.73	NA
ESP_033713†	05 Oct 2013	31.4°	MY32 sp.	18°	189.3°	6.4°	45.0°	1.33	0.40
ESP_033766	09 Oct 2013	33.3°	MY32 sp.	18°	196.8°	7.0°	44.4°	1.31	0.12
ESP_034254	16 Nov 2013	50.3°	MY32 sp.	24°	202.8°	4.7°	55.2°	1.44	0.29
ESP_034399	27 Nov 2013	55.3°	MY32 sp.	25°	202.6°	4.7°	55.2°	1.55	0.18
ESP_034610	14 Dec 2013	62.5°	MY32 sp.	27°	205.0°	4.7°	55.2°	1.57	0.16
ESP_053730	12 Jan 2018	113.9°	**MY34 su.**	28°	197.4°	6.4°	45°	1.80	NA
ESP_069095	23 Apr 2021	35.5°	MY36 sp.	19°	198.0°	4.7°	55.2°	1.24	0.56
ESP_069649	5 Jun 2021	54.7°	MY36 sp.	25°	202.0°	4.7°	55.2°	1.49	0.31
ESP_069834	19 Jun 2021	61.0°	MY36 sp.	25°	202.0°	4.7°	55.2°	1.54	0.26
ESP_069992	2 Jul 2021	66.4°	MY36 sp.	31°	202.0°	4.7°	55.2°	1.61	0.19

* Image ID should be suffixed with "_2650". † marks the images with a grid size of 0.50 m, while the rest of them feature a better resolution of 0.25 m. Note that the solar azimuth is with respect to the North Pole while the slope aspect is defined as the angle with respect to the map north. sp. is the abbreviation for spring and su. for summer. Summer images used to derive the reference heights are marked in bold.

Table S4: Statistical Summary of the Thickness of the Seasonal Deposits in Late Winter and Spring of MY31

Thickness [m]	Solar Longitude								
	350.7°	7.0°	17.3°	22.7°	30.3°	35.4°	42.8°	55.1°	69.5°
Snowfall	0.97±0.13	0.64±0.08	0.54±0.03	0.50±0.08	0.46±0.05	0.41±0.06	0.21±0.05	0.13±0.05	0.02±0.02
Frost	0.64±0.18	0.49±0.09	0.42±0.06	0.41±0.04	0.33±0.07	0.25±0.03	0.26±0.03	0.12±0.02	0.05±0.04
Sum	1.63±0.22	1.12±0.12	0.96±0.07	0.92±0.09	0.79±0.09	0.64±0.07	0.45±0.06	0.25±0.05	0.06±0.05

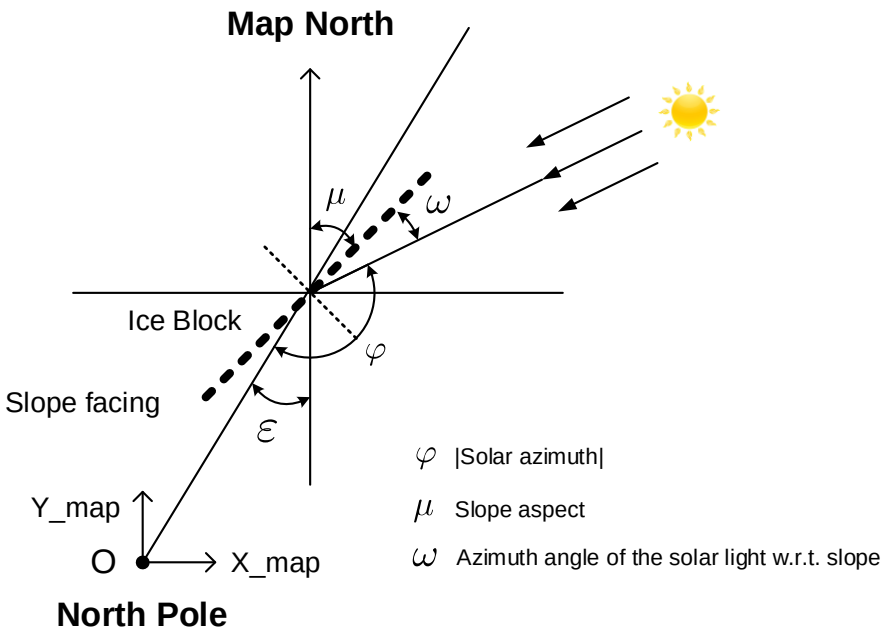

Figure S1: Schematic that illustrates the measured slope aspect and solar azimuth, and their relation to ω, which represents the angular separation between the solar rays and the bearing of the slope. Origin of the map coordinate system, associated with a polar stereographic projection, centers at the North Pole.

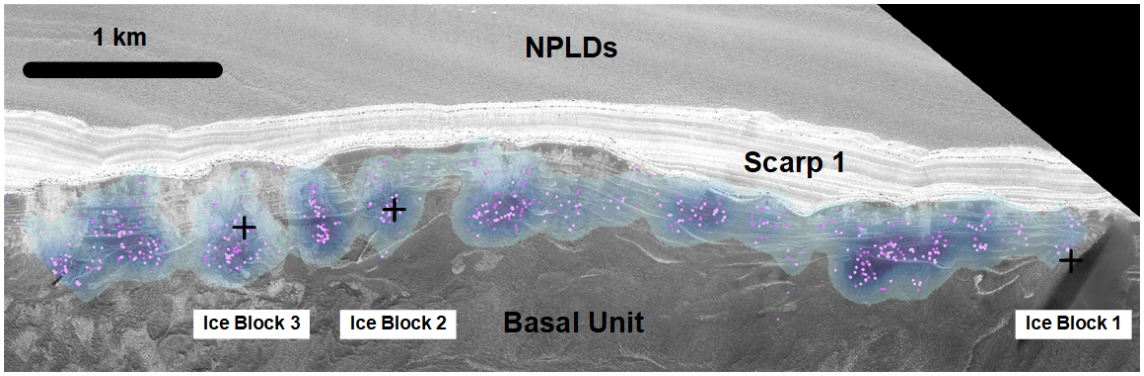

Figure S2: Distribution of the selected bounding ice blocks used to constrain the depth evolution of the seasonal deposits in MY31. Location is at Scarp 1, which is centered at (85.0°N, 151.5°E). Background image is a summer image acquired in MY29 (`PSP_009648_2650_RED`; same as that used in Figure 3). Ice blocks that have been completely covered are marked by points in dark purple, while ice blocks that have not been submerged are marked by points in light purple. These points are draped over the density map with darker tone represents higher degree of clustering of the points. We mark the locations of Ice Blocks 1, 2, and 3 for reference.

Text S1. Probabilistic analysis on the number of iterations needed in the self-registration of the MOLA profiles

Here, we discuss how many iterations are needed in the self-registration of the MOLA profiles with the aim to generate a reference topographic model of the Martian North Pole. The probability that a specific profile, out of a full set of N profiles, has not ever been selected and co-registered throughout all n iterations performed is

$$p = (1 - p_s)^n \,, \tag{1}$$

where $p_s = 0.25$ is the fraction of the profiles randomly chosen at each iteration to be co-registered to the rest of the profiles. The probability that a specific profile has been selected for co-registration for at least once then stands at $q = 1 - p$. We now define a discrete random variable X that describes the number of profiles that have not ever been co-registered in the random selection process. Then, X follows the binomial distribution, $X \sim \mathrm{B}(N, p)$, which represents the number of successes in a sequence of N independent Bernoulli trials, each with a success rate of p. The probability mass function is as follows:

$$\mathbb{P}(X = k) = \frac{N!}{k!(N-k)!} p^k q^{N-k} \quad (k = 0,\, 1,\, 2,\, \ldots,\, N) \,, \tag{2}$$

where ! is the factorial function and k denotes the number of profiles that have not been co-registered after n iterations. Given that N is sufficiently large ($\gg 20$) and that p is small ($\ll 0.05$), X can be approximated by a Poisson distribution $X \sim \mathrm{Pois}(\lambda)$, which has a probability mass function given by

$$\mathbb{P}(X = k) = \frac{\lambda^k e^{-\lambda}}{k!} \quad (k = 0,\, 1,\, 2,\, \ldots,\, N) \,, \tag{3}$$

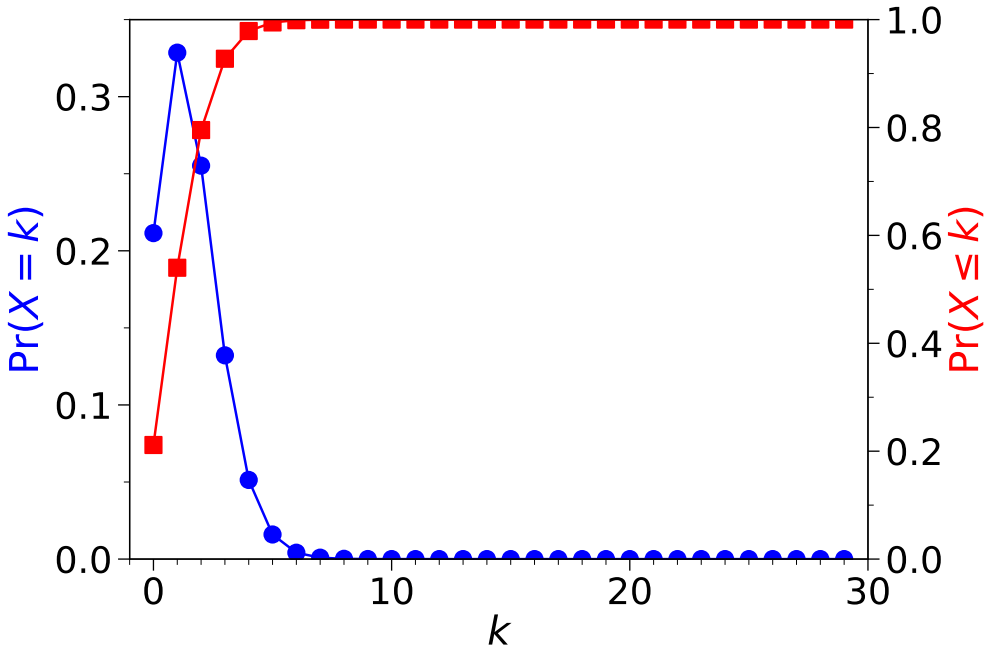

Figure S3: The probability mass function (blue dots) and cumulative distribution function (red squares) of the random variable X using $N = 8,700$ and $n = 30$.

where e is Euler's number and the positive number λ equals the expected value of X, that is, $\lambda = Np$. The cumulative distribution function of the integer-valued random variable X is

$$\mathbb{P}(X \leq k) = e^{-\lambda} \sum_{m=0}^{k} \frac{\lambda^m}{m!} = \frac{\Gamma(k+1,\, \lambda)}{k!}\,, \tag{4}$$

where $\Gamma(k+1,\, \lambda)$ is the upper incomplete gamma function. In the MOLA case of a total number of 8,700 profiles, that is $N = 8,700$, and 30 iterations, that is $n = 30$, the most probable number of profiles that have not been co-registered even once stand at just one, with a probability of 0.33 (Figure S3). Meanwhile, the cumulative probability that less than 6 profiles have not been co-registered in the self-registration iterations reaches 99.88%. These statistics justify the repeating of the self-registration process for up to 30 times.